Machine Learning-Assisted Quasi-Bisection Method for Pixelated Patch Antenna Bandwidth Optimization

Qipeng Wang, Zhongxuan Pang, Di Gao, Peng Liu, Xiaoyu Pang, and Xiaoxing Yin, *Member, IEEE*

***Abstract*—A machine learning-assisted quasi-bisection method (MLAQBM) is proposed for the broadband optimization of the pixelated patch antennas. Distinct from traditional MLA optimization methods, MLAQBM employs a coarse-to-fine pixel partition and machine learning optimization to iteratively refine the shape of the antenna. Two implementation strategies are introduced. In the first strategy, larger pixels are initially partitioned and samples are collected. A surrogate model is then established using convolutional neural networks (CNN), and an initial shape is derived through particle swarm optimization (PSO). Again, further refinement is achieved by finer pixel partitioning and subsequent CNN-based PSO. The second strategy leverages a pre-existing broadband E-shaped patch design, which is then subdivided into smaller pixels. By collecting samples, training a CNN surrogate model, and performing PSO optimization, a broader bandwidth is realized. Compared with the reported MLA optimization methods, MLAQBM establishes a stable surrogate model that is robust, easy to converge, and adaptable to different optimization objectives. To validate the proposed strategies, the optimized pixelated patch antennas are fabricated and measured. The measured results demonstrate that the bandwidth of the proposed patch antennas achieves 24.5% and 32.5%.**

***Index Terms*—Antennas, convolutional neural network (CNN), machine learning, particle swarm optimization (PSO), pixel, quasi-bisection method.**

I. Introduction

With the rapid development of modern communication, broadband antenna design has emerged as a critical evolution [1]. Pixelated design, which involves partitioning a metal patch into sufficiently small units and optimizing the presence or absence of metal within these units, is an effective approach for realizing broadband antennas [2], [3]. However, conventional designs suffer from a lack of a priori knowledge and a wide optimization space. Machine learning-assisted optimization (MLAO) methods benefit from high efficiency and excellent performance [4], [5], [6], [7]. However, a surrogate model that is capable of completely characterizing greater than 2^{40} pixel variations is difficult to train [8], [9], [10]. Therefore, an MLAO method that can precisely surrogate pixelated antenna and efficiently accelerate optimization is in high demand.

Received 23 September 2024; accepted 4 October 2024. Date of publication 7 October 2024; date of current version 13 December 2024. *(Corresponding author: Qipeng Wang.)*

Qipeng Wang, Zhongxuan Pang, Di Gao, Peng Liu, and Xiaoyu Pang are with the Aeronautical Science Key Laboratory for High Performance Electromagnetic Windows, AVIC Research Institute for Special Structures of Aeronautical Composites, Jinan 250023, China (e-mail: wqpseu637@163.com).

Xiaoxing Yin is with the State Key Laboratory of Millimeter Waves, Southeast University, Nanjing 210096, China.

Digital Object Identifier 10.1109/LAWP.2024.3475628

Recently, several MLAO methods have been demonstrated in accelerating optimization iterations for pixelated patch antenna design [8], [9], [10], [11]. For instance, Gaussian process regression (GPR) with small datasets for initial surrogate model training, which is then optimized iteratively using a differential evolutionary algorithm (DEA) [8], [11]. Moreover, pixelated patch antennas that satisfy the design objectives can also be achieved by EAs after extensive continuous iterative evaluations of the function [9], [10]. Although the aforementioned method effectively reduces the number of required samples, it exhibits low robustness. When the optimization objective changes, there is a high likelihood that the optimization must be performed from the beginning.

An MLA quasi-bisection method (QBM) is proposed for the broadband optimization of the pixelated patch antennas. The novelties of the MLAQBM are summarized as follows.

1) Hierarchical optimization strategy. The proposed MLAQBM employs a coarse-to-fine optimization methodology. Coarse pixels are utilized to establish a preliminary model, while finer pixels subsequently refine the optimization, thereby enhancing the overall efficiency of the design process.
2) Relatively high robustness. The training of the surrogate model relies on randomly sampled data, enhancing its stability and making it suitable for various optimization objectives.

II. MLAQBM Framework

Binary search is an efficient algorithm for finding a specific element in a sorted array. It narrows down the search range by halving the search interval each time, comparing the middle element with the target value to determine which half to continue searching [12]. Inspired by the concept of binary search [12], the framework of the proposed MLAQBM is illustrated in Fig. 1. To improve the optimization efficiency and reduce the computational cost, a two-stage MLAQBM optimization strategy is adopted as a typical example. The specific process of realization of each stage is summarized as follows:

Stage I: Initial Design and Exploration

Initially, the patch is divided into m $\times$ n equally sized rectangles, similar to pixel blocks. Subsequently, these pixel blocks are represented by "0" and "1," where "1" denotes metal and "0" denotes air. A randomly selected m $\times$ n binary matrix X is then obtained to characterize the pixelated patch antenna.

The random sampling approach ensures comprehensive exploration of the design space, maintains computational

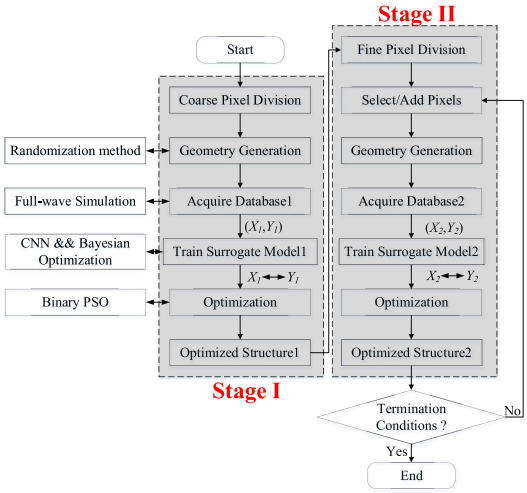

Fig. 1. Framework of the proposed MLAQBM.

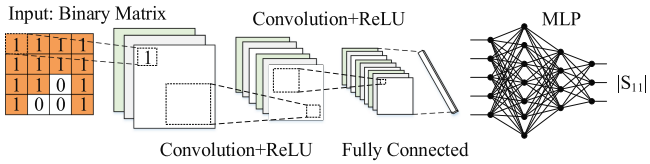

Fig. 2. Framework of the surrogate model.

efficiency and facilitates accurate surrogate model training for effective optimization. Utilizing Python to invoke CST Studio Suite, the m × n binary matrix is converted into an EM model for full-wave simulation. Due to the superior handling of high-dimensional data and complex relationships, a convolutional neural network (CNN) is selected for the surrogate model. With convolutional layers, CNN can reduce dimensionality and extract pixel features. Combined with multilayer perceptron (MLP), the nonlinear mappings between pixel configurations and reflection coefficients can be captured. Therefore, the m × n binary matrix is employed as the input of the CNN, while the reflection coefficients of the patch antenna Y serve as the output of the MLP, as depicted in Fig. 2.

$$Y = [y_1 \quad y_2 \quad \cdots \quad y_k] \tag{1}$$

where k indicates that k frequency points are selected at equal intervals.

Bayesian hyperparameter optimization is adopted in MLP to obtain a surrogate model 1 for the m × n pixelated patch antenna. To achieve a broader bandwidth, the binary particle swarm optimization (PSO) algorithm is used based on the surrogate model. The fitness of the binary PSO algorithm is

$$Y_{st} = \min(\max(y_i)), \quad i = s, s+1, \cdots, t \tag{2}$$

where y_i represents the reflection coefficient in the passband. The selection of discrete frequency samples within the desired band allows for targeted optimization, ensuring the reflection coefficients across the frequency range remain below the specified threshold, thereby expanding the bandwidth.

Stage II: Refinement and Optimization

Based on the antenna structure optimized in Stage I, the patch is further subdivided into 2m × 2n smaller pixels. The search

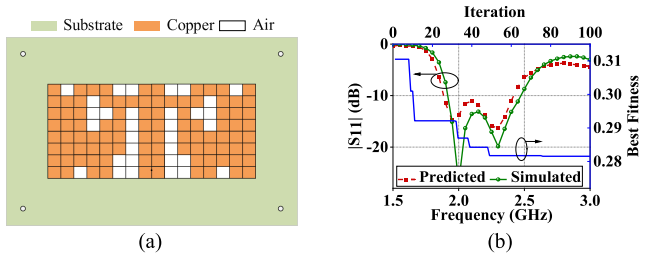

Fig. 3. (a) Top view of the pixelated patch antenna. (b) Reflection coefficients of predicted and simulated 8 × 8 pixelated patch antennas and fitness of PSO.

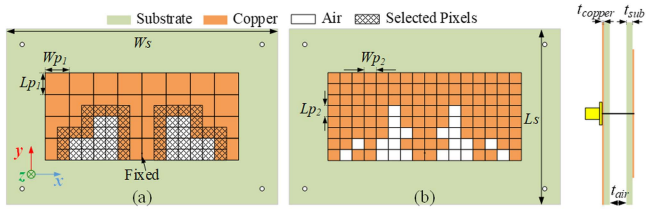

Fig. 4. (a) Top view of the large pixelated patch antenna. (b) Top view of the small pixelated patch antenna. Dimensions (mm): $Ws = 140$, $Ls = 90$, $Wp_1 = 12.5$, $Lp_1 = 11.25$, $Wp_2 = 6.25$, $Lp_2 = 5.625$, $t_{sub} = 1.524$, $t_{copper} = 0.018$, $t_{air} = 8$.

space is expanded around the rectangles currently designated as "0." Random selection is used for the areas chosen for expansion, while the regions outside the selected area continue to retain the pixel value of "1." Since the selected area is smaller compared to the complete set of 2m × 2n pixels, it is easier to train and establish a surrogate model 2. With the surrogate model 2, the binary PSO algorithm can efficiently achieve a broadband pixelated patch antenna

III. Application to Pixelated Patch Antenna

A. Hierarchical MLAQBM Optimization

To reduce cross-polarization and simplify the design, pixelated patch antennas typically employ a symmetrical layout [8], [9], [10]. In addition, certain positions are normally fixed to ensure the stability of the probe feed. For comparison, the patch antenna divided into 8 × 8 pixels is trained initially based on CNN in Fig. 2. Fixed pixels are not selected, and all other pixels are randomly sampled. The 24 373 sets of samples are collected, and the CNN-based surrogated model is trained. The training and testing mean relative error (MRE) are 18.57% and 23.83%, respectively. Optimization is performed using binary PSO based on a surrogate model. Consequently, the configuration of the optimized patch is plotted in Fig. 3(a). The predictions and the simulation results as illustrated in Fig. 3(b). The optimized bandwidth is 25.6%.

For MLAQB, the patch antenna is divided into 4 × 8 large pixels, half of which are represented by a binary matrix and input into the CNN as shown in Fig. 4(a). The patch antenna utilizes the classic dual-layer RO4003C dielectric substrate with a bottom-fed probe [13]. The substrates are separated by nylon spacers. A total of 2500 sets of 4 × 4 binary matrices are generated. CNN is utilized as the surrogate model, in which the node counts for the MLP are determined by Bayesian hyperparameter optimization, set at 208, 256, and 110, respectively. The training

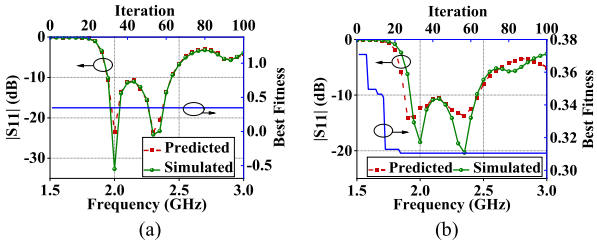

Fig. 5. Reflection coefficient of the optimized pixelated patch antenna predicted by the surrogate model and simulated by CST Studio Suite as well as the fitness of the binary PSO. (a) Stage I (b) Stage II.

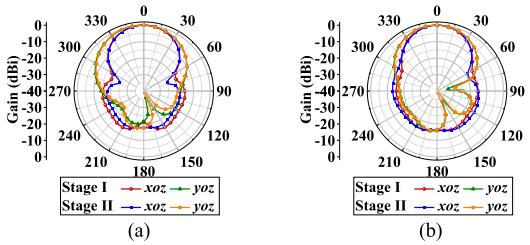

Fig. 6. Radiation pattern at two resonant frequencies. (a) 2 GHz. (b) 2.34 GHz.

MRE and testing MRE are 3.14% and 5.88%, respectively. The training dataset size over the total sample space is 7.62%. The combination of data splitting, validation set monitoring, dropout layers, and early stopping is employed to prevent overfitting, ensuring the model maintains strong generalization capabilities during the training process.

The optimization is performed by combining the surrogate model and the binary PSO. It should be noted that to improve the efficiency of optimization, the 50 samples with the widest bandwidth from the collected data are chosen as the initial samples for the PSO. The predicted results of the surrogate model, the EM simulation results, and the fitness of the PSO are shown in Fig. 5(a).

Based on the optimization from Stage I, the pixels are further refined, expanding the selection area around non-metal pixels. The grid area shown in Fig. 4(a) represents the selected variable pixels for Stage II. The other pixels remain set to "1." After randomly sampling 3533 sets, the 8×8 binary matrices and corresponding reflection coefficients are inputted into CNN to establish surrogate model 2. The optimized node counts for the MLP are 256, 256, and 105, respectively. The training MRE and testing MRE are 5.23% and 13.66%, respectively. The training dataset size over the total sample space is 0.0053%. Optimization is performed using Binary PSO based on surrogate model 2. The optimized structure of the antenna is shown in Fig. 4(b). The comparison between the reflection coefficients predicted by surrogate model 2 and the EM simulation results, and the fitness of the PSO are presented in Fig. 5(b). Compared to Stage I, the bandwidth in Stage II increased by 5%. The radiation patterns at two resonant frequencies are illustrated in Fig. 6, from which no significant change can be observed.

B. MLAQBM With Prior Design Knowledge

Various patch shapes have been explored over the past decades to enhance the bandwidth of patch antennas [14], [15], [16], [17].

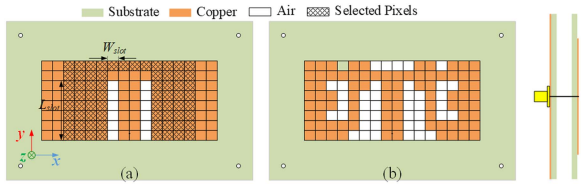

Fig. 7. (a) Top view of the E-shaped patch antenna. (b) Top view of the small pixelated patch antenna. Dimensions (mm): $W_{slot} = 6.25$, $L_{slot} = 33.75$.

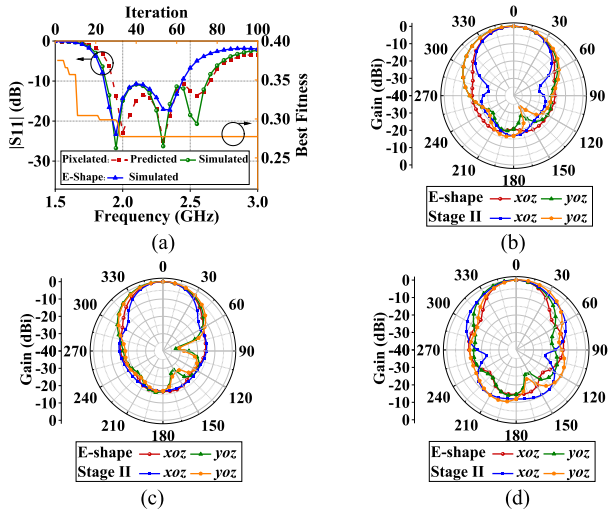

Fig. 8. (a) Reflection coefficient of the optimized pixelated patch antenna predicted by the surrogate model and simulated by CST Studio Suite, as well as the fitness of the binary PSO. (b) Radiation pattern at 1.95 GHz. (c) 2.3 GHz. (d) 2.52 GHz.

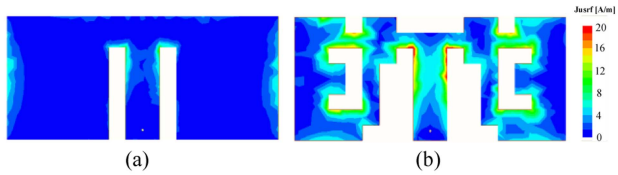

Fig. 9. Current distribution at 2.52 GHz. (a) Conventional E-patch antenna. (b) Optimized pixelated patch antenna.

The typical E-shaped patch is taken as the optimization result of Stage I, as shown in Fig. 7(a). In this case, the bandwidth can be further extended by selecting variable pixels and stepping into Stage II. The E-shaped main structure is retained and the surrounding metal area is chosen as a variable pixel as depicted in Fig. 7(a). The optimized node counts for the MLP are 303, 382, 203, and 224, respectively. The training MRE and test MRE are 10.2% and 17.7%, respectively. The training dataset size over the total sample space is 0.000028%. The optimized structure of the pixelated patch antenna is shown in Fig. 7(b). The reflection coefficients of the E-shaped patch and the optimized pixelated patch are shown in Fig. 8(a), where the latter one introduces a third mode at 2.52 GHz. The bandwidth of the pixelated patch is increased from 27% to 32.5% compared with the E-shaped one. The radiation patterns of the two antennas at different resonant frequencies are simulated in Fig. 8(b)–(d). To investigate the modal behaviors of this new resonant mode, the current distributions at 2.52 GHz as shown in Fig. 9. The optimized antenna shows a much higher current density and

TABLE I
COMPARISON BETWEEN THE PROPOSED AND STATE-OF-THE-ART PIXELATED ANTENNA

Method	Surrogate Model	Initial Sample Dependency	Training Samples	Time (h)	Computational Complexity	BW (%)	Robustness
MLAO-DEA [8]	Yes	High	> 50	> 9.62	$O(N_{ini}\times T_{sim}+T\times N\times T_{fit}+N_{up}\times T_{sim})$	23.2	Moderate
BSO [9]	No	Moderate	6000	N. A.	$O(T\times(N\times D+N\times D\times M+N\times logN+N\times T_{sim}))$	23.2	Bad
GA [10]	No	Moderate	52000	32	$O(T\times N\times T_{fit})$	5.3, 7	Bad
Cross-Entropy [18]	No	Moderate	N. A.	<16.6	$O(T\times N\times D\times T_{sim})$	N. A.	Bad
NSGA-II [19]	Yes	Low	N. A.	N. A.	$O(T\times N\times T_{fit})$	13.8	Moderate
SEBO [20]	Yes	Low	N. A.	N. A.	$O(2^{Jmax})$	7.3, 16.8	Moderate
Without QBM	Yes	Low	24373	236.97	$O(N_{samples}\times T_{sim}+N_{samples}\times T_{train}+N\times T\times T_{fit})$	25.6	Good
This Work MLAQBM	Yes	Low	2500 & 3533	58.65	$O((N_{samples1}\times T_{sim}+N_{samples1}\times T_{train}+N\times T\times T_{fit})+$	24.5	Good
			4382	42.60	$(N_{samples2}\times T_{sim}+N_{samples2}\times T_{train}+N\times T\times T_{fit}))$	32.5	Good

N. A. represents not available. N_{ini} is the number of initial samples, T_{sim} is the electromagnetic simulation time of each solution, T is the total iterations number, N is the population size, T_{fit} is the fitness evaluation time using the surrogate model, N_{up} is the number of updates of the surrogate model, D is number of design variables, M is the number of clusters, J_{max} is number of variables per pixel, $N_{samples}$ is number of samples and T_{train} is the training time of the surrogate model.

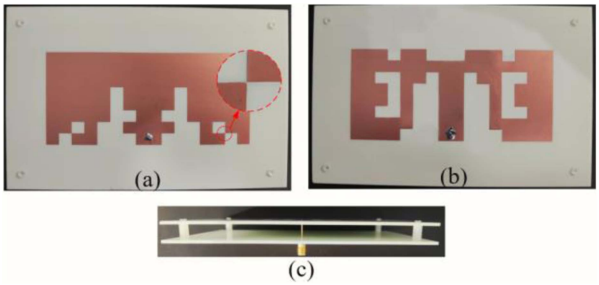

Fig. 10. Prototype of the proposed pixelated patch antennas (a). Top view of the hierarchical MLAQBM optimized one. (b) Top view of the prior design knowledge-based one. (c) Side view.

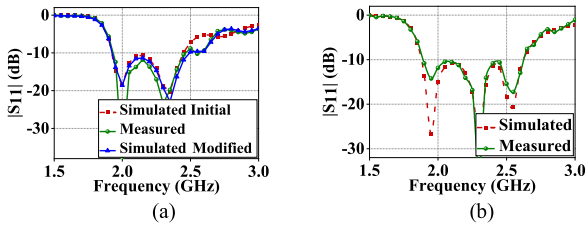

Fig. 11. Simulated and measured reflection coefficient of the pixelated patch antennas. (a) Hierarchical MLAQBM optimized one. (b) Prior design knowledge-based one.

better current concentration at sharp edges, corners, and the edge of the U-slot, which should contribute to improved radiation. This characteristic is also reflected in a lower $|S_{11}|$ value at 2.52 GHz.

IV. EXPERIMENTAL VALIDATION

To validate the proposed method, prototypes of the pixelated patch antennas investigated above are fabricated, as shown in Fig. 10. The classic dual-layer RO4003C dielectric substrate with a bottom-fed probe is adopted for the pixelated patch antennas. The substrates are separated by nylon spacers for wider operating bandwidth. The thickness of the copper cladding is set to 18 μm. The patch antennas are simulated by CST Studio Suit and measured utilizing an Agilent vector network analyzer (VNA). The simulated and measured reflection coefficients of the patch antennas are depicted and compared in Fig. 11. In Fig. 11(a), the reflection coefficients of the Hierarchical MLAQBM optimized pixelated patch antenna remain below −10 dB from 1.93 GHz to 2.47 GHz, achieving a relative bandwidth of 24.5%. Due to poor manufacturing, one of the vertices is broken off, as shown in Fig. 10(a). Disconnection at the vertices results in a variance of the current path, changing the impedance matching of the antenna. Thereby, modifications of the simulation model are performed and the simulation results are obtained, as shown in Fig. 11(a). Compared with the measured results, a relatively good agreement can be observed. In addition, the prior design knowledge-based one features reflection coefficients better than −10 dB from 1.88 GHz to 2.61 GHz, resulting in a bandwidth as high as 32.5%, as shown in Fig. 11(b).

A comparison between the proposed and state-of-the-art pixelated antenna is summarized in Table I. The DEA-based method is capable of updating the surrogate model during the optimization process [8]. However, these methods typically require high-quality initial training samples. Although some EA or probabilistic algorithms demonstrate the capability to iteratively optimize a target result within hours, the robustness is poor [9], [10], [18]. Even minor changes in the optimization objective necessitate restarting the entire optimization process. In [19], [20], the internal multiport method (IMPM) is employed as an efficient surrogate model for extracting network parameters between patches and predicting antenna performance in different connection states. Nevertheless, the tight connection between the pixels of the proposed patch antenna limits the application of IMPM. Compared with the one without QBM, the proposed MLAQBM involves fewer training samples, shorter optimization times, and higher efficiency. The training of the proposed surrogate model relies on randomly sampled data, enhancing its stability and making it suitable for various optimization objectives.

V. CONCLUSION

In this letter, an MLAQBM is proposed for the broadband optimization of the pixelated patch antennas. Two implementation strategies with two stages are introduced. In each stage, a CNN is utilized to obtain a surrogate model, and PSO is employed to optimize the structural parameters for wideband design.

REFERENCES

[1] R. Cicchetti, E. Miozzi, and O. Testa, "Wideband and UWB antennas for wireless applications: A comprehensive review," *Int. J. Antennas Propag.*, vol. 2017, pp. 1–45, 2017.

[2] G. Kumar and K. P. Ray, *Broadband Microstrip Antennas.* Norwood, MA, USA: Artech House, 2002.

[3] S. Targonski, R. Waterhouse, and D. Pozar, "Design of wide-band aperture-stacked patch microstrip antennas," *IEEE Trans. Antennas Propag.*, vol. 46, no. 9, pp. 1245–1251, Sep. 1998.

[4] J. Zhang, M. O. Akinsolu, B. Liu, and S. Zhang, "Design of zero clearance SIW endfire antenna array using machine learning-assisted optimization," *IEEE Trans. Antennas Propag.*, vol. 70, no. 5, pp. 3858–3863, May 2022.

[5] D. Sarkar, T. Khan, Jayadeva, and A. A. Kishk, "Machine learning assisted Hybrid electromagnetic modeling framework and its applications to UWB MIMO Antennas," *IEEE Access*, vol. 11, pp. 19645–19656, 2023.

[6] Y. Su et al., "Time-domain scattering parameters based neural network inverse model for antenna designs," *IEEE Antennas Wireless Propag. Lett.*, vol. 23, no. 7, pp. 1976–1980, Jul. 2024.

[7] B. Karaosmanoglu and O. Ergul, "Visual result prediction in electromagnetic simulations using machine learning," *IEEE Antennas Wireless Propag. Lett.*, vol. 18, no. 11, pp. 2264–2266, Nov. 2019.

[8] Q. Wu, W. Chen, C. Yu, H. Wang, and W. Hong, "Machine-learning-assisted optimization for antenna geometry design," *IEEE Trans. Antennas Propag.*, vol. 72, no. 3, pp. 2083–2095, Mar. 2024.

[9] A. Aldhafeeri and Y. Rahmat-Samii, "Brain storm optimization for electromagnetic applications: Continuous and discrete," *IEEE Trans. Antennas Propag.*, vol. 67, no. 4, pp. 2710–2722, Apr. 2019.

[10] F. J. Villegas, T. Cwik, Y. Rahmat-Samii, and M. Manteghi, "A parallel electromagnetic genetic-algorithm optimization (EGO) application for patch antenna design," *IEEE Trans. Antennas Propag.*, vol. 52, no. 9, pp. 2424–2435, Sep. 2004.

[11] B. Liu, H. Aliakbarian, Z. Ma, G. A. E. Vandenbosch, G. Gielen, and P. Excell, "An efficient method for antenna design optimization based on evolutionary computation and machine learning techniques," *IEEE Trans. Antennas Propag.*, vol. 62, no. 1, pp. 7–18, Jan. 2014.

[12] W. H. Press, *Numerical Recipes 3rd Edition: The Art of Scientific Computing*. Cambridge, U.K.: Cambridge Univ. Press, 2007.

[13] D. M. Pozar, "Microstrip antennas," *Proc. IEEE*, vol. 80, no. 1, pp. 79–91, Jan. 1992.

[14] F. Yang, X.-X. Zhang, X. Ye, and Y. Rahmat-Samii, "Wide-band E-shaped patch antennas for wireless communications," *IEEE Trans. Antennas Propag.*, vol. 49, no. 7, pp. 1094–1100, Jul. 2001.

[15] R. Chair, C. L. Mak, L. Kai-Fong, L. Kwai-Man, and A. A. Kishk, "Miniature wide-band half U-slot and half E-shaped patch antennas," *IEEE Trans. Antennas Propag.*, vol. 53, no. 8, pp. 2645–2652, Aug. 2005.

[16] J.-D. Zhang, W. Wu, and D.-G. Fang, "Dual-band and Dual-circularly polarized shared-aperture array antennas with single-layer substrate," *IEEE Trans. Antennas Propag.*, vol. 64, no. 1, pp. 109–116, Jan. 2016.

[17] Y. He, J. Huang, W. Li, L. Zhang, S.-W. Wong, and Z. N. Chen, "Hybrid method of artificial neural network and simulated annealing algorithm for optimizing wideband patch antennas," *IEEE Trans. Antennas Propag.*, vol. 72, no. 1, pp. 944–949, Jan. 2024.

[18] M. Kovaleva, D. Bulger, and K. P. Esselle, "Cross-entropy method for design and optimization of pixelated metasurfaces," *IEEE Access*, vol. 8, pp. 224922–224931, 2020.

[19] F. Peng, C. Liao, Y.-F. Cheng, J. Feng, X.-W. Mo, and X. Ding, "Design and optimization of a high-gain filtering antenna based on parasitic pixel layer," *EEE Antennas Wireless Propag. Lett.*, vol. 22, no. 5, pp. 1104–1108, May 2023.

[20] S. Shen, Y. Sun, S. Song, D. P. Palomar, and R. D. Murch, "Successive Boolean optimization of planar pixel antennas," *IEEE Trans. Antennas Propag.*, vol. 65, no. 2, pp. 920–925, Feb. 2017.